DEUTSCHES ELEKTRONEN-SYNCHROTRON DESY

DESY 85-089
August 1985

T SPECTROSCOPY

by

Kay Königsmann
Universität Würzburg, 8700 Würzburg, Germany
and
Deutsches Elektronen-Synchrotron DESY, Hamburg, Germany

ISSN 0418-9833

NOTKESTRASSE 85 · 2 HAMBURG 52

To be sure that your preprints are promptly included in the
HIGH ENERGY PHYSICS INDEX ,
send them to the following address (if possible by air mail) :

DESY
Bibliothek
Notkestrasse 85
2 Hamburg 52
Germany

DESY 85-089
August 1985

ISSN 0418-9833

Υ Spectroscopy

Kay Königsmann

Universität Würzburg
8700 Würzburg, Germany
and
Deutsches Elektronen-Synchrotron DESY
2000 Hamburg, Germany

ABSTRACT. A summary is presented on radiative decays of the $\Upsilon(1S)$ and $\Upsilon(2S)$ states as measured by the detectors ARGUS, CLEO, Crystal Ball and CUSB operating at the storage rings CESR and DORIS II. In particular, the search for heavy mass states below the $\Upsilon(1S)$ resonance is discussed. Nothing (un)expected in the form of gluonium, supersymmetric particles or Higgs bosons has shown up yet. Also covered are transitions from the $\Upsilon(2S)$ resonance to the ${}^3P_J$ bottonium states which have been measured with high precision. The spins of those states are shown to be consistent with expectation. Comparison with potential models yields information on the inter-quark force. It is argued that the Υ states are an ideal testing ground for the theory of strong interactions.

Invited talk presented at the 5th International Conference on Physics in Collision; Autun, France, July 3-5 1985.

Introduction

Over the last ten years much of the theoretical and experimental investigation of the physics of elementary particles has been devoted to the study of heavy quark systems consisting of bound $c\bar{c}$ and $b\bar{b}$ quarks. They prove an ideal laboratory to study three of the forces acting on elementary particles: the strong, electromagnetic and weak force in the Standard Model[1] of High Energy Physics. Weak decays of heavy quark-antiquark ($Q\bar{q}$) bound states above the open flavor threshold are used to study the electroweak interactions. Below this threshold $b\bar{b}$ states are a testing ground for the theory of strong interactions, Quantum Chromodynamics[2] (QCD). Two main areas of research for the $b\bar{b}$ resonances offer themselves: their decay properties and their mass spectra. In both areas photon transitions play an important role. They reveal the predicted C-even $c\bar{c}$ and $b\bar{b}$ ${}^3P_J$ states, and allow us either to search for transitions to well known $q\bar{q}$ mesons like η, η' *etc.* or to hunt for new states in form of gluonium,[3] supersymmetric particles[4] and Higgs bosons.[5]

In this report we will discuss experimental results obtained by investigating the radiative decays of the two lowest mass resonances, the $\Upsilon(1S)$ and the $\Upsilon(2S)$. These resonances consist of a b and a $\bar{b}$ quark in a relative ${}^3S_1$ state. As the spin-parity of these states is the same as that of the photon ($J^{PC} = 1^{--}$), they are produced directly in e^+e^- collisions. Radiative decays of these states thus allow to obtain information on C-even states. We discuss in detail the search for high mass resonances in radiative decays of the $\Upsilon(1S)$ as well as the observation of the ${}^3P_J$ states of bottonium found in transitions from the $\Upsilon(2S)$.

Detectors

The data to be discussed here were obtained by the experiments CLEO[6] and CUSB[7] operating at the storage ring CESR (Cornell) and by ARGUS[8] and Crystal Ball[9] situated at the DORIS II storage ring in Hamburg. Both e^+e^- colliding machines are very well suited for a study of the bottonium system in the center-of-mass energy region around 10 GeV. Due to its bigger radius the CESR machine provides a center-of-mass energy resolution superior to DORIS' by nearly a factor of two ($\simeq 4$ MeV vs. $\simeq 8$ MeV). For narrow resonances like the $\Upsilon(1S)$, $\Upsilon(2S)$ and $\Upsilon(3S)$ equal luminosities result in higher event rates by about a factor of two and correspondingly lower background contributions from non-resonant e^+e^- interactions for the CESR experiments.

The experiments operating at these machines can be classified into two categories: magnetic (ARGUS and CLEO) and non-magnetic (Crystal Ball and CUSB) detectors. Both magnetic detectors are of the general-purpose type employing a high magnetic field, good charged particle tracking and momentum measurement using drift-chambers, and fair energy

resolution for electromagnetically showering particles using shower calorimeters (see Table 1). As the resolution of these shower counters is not sufficient to obtain a precise energy determination for photons, magnetic detectors employ the technique of fitting e^+e^- pairs from converted photons. The conversion may take place either in the beam-pipe plus the inner wall of the drift-chamber or in a specially installed lead converter close to the beam-pipe (CLEO). Little material in front of the drift-chamber offers the advantage of a very precise energy measurement at the cost of efficiency for detecting photons. We will see below that the two magnetic detectors followed different approaches to optimize photon detection in inclusive events.

	ARGUS	CLEO	CRYSTAL BALL	CUSB
Magnetic Field	0.8 T	1.0 T	· / ·	· / ·
σ_p/p (%)	$\approx 1.2 \times p$	$\approx 1.2 \times p$	· / ·	· / ·
σ_E/E (%)	$(7^2 + 8^2/E)^{1/2}$	$17 \;/\; E_{GeV}^{1/2}$	$2.7 \;/\; E_{GeV}^{1/4}$	$4 \;/\; E_{GeV}^{1/4}$
σ_{E_γ} at 100 MeV	1.1 MeV	2.5 MeV	4.8 MeV	7.1 MeV
σ_{E_γ} at 1 GeV	10 MeV	12 MeV	27 MeV	40 MeV (*NaI*) 19 MeV (*BGO*)
ϵ_γ at 100 MeV	0.2 %	2 %	15 %	13 %
ϵ_γ at 1 GeV	2 %	3 %	15 %	13 %

TABLE 1
Detector parameters relevant to inclusive and exclusive photon measurements. σ_p refers to the momentum resolution for charged tracks obtained using drift chambers only. σ_E is the energy resolution for electromagnetically showering particles in the shower counters. For the detector-specific approaches to inclusive analyses (see text), typical resolution (σ_γ) and efficiency (ϵ_γ) values at two energies are included.

The non-magnetic detectors are optimized for high resolution measurements of electromagnetically showering particles and are thus ideal for the study of inclusive and exclusive events containing an arbitrary number of photons. Following a drift chamber for charged particle tracking, Crystal Ball and CUSB employ a highly segmented array of sodium iodide scintillators. The Crystal Ball NaI detector with its 16 radiation lengths (X_0) contains electromagnetic showers to a very good degree. The CUSB calorimeter is only $9X_0$ deep and therefore is backed with lead glass Čerenkov counters to fully contain the showers. The latest CUSB results on the $\Upsilon(1S)$ radiative decays have been obtained with a newly installed BGO (Bismuth Germanate, $Bi_4Ge_3O_{12}$) quadrant in place of the drift chamber. This is the first operating BGO detector in a High Energy Physics experiment. In Table 1 we summarize

those features of the detectors relevant to analyses of radiative decays.

To appreciate the quite different behaviour of the two types of detectors we sketch in Fig. 1 the typical photon energy resolution functions and photon detection efficiencies for the analysis of inclusive photons in a hadronic environment. The superior energy resolution of both magnetic detectors is apparent. The shower detectors on the other side feature a very high efficiency to detect such photons. Therefore we may expect the results from both detector classes to be partly complementary: high statistical significance and thus small errors on the branching ratios from the shower detectors, while the magnetic detectors will supply us with a very accurate photon energy measurement and thus mass determination of the final state. Due to the very small detection efficiency magnetic detectors are not in a position to detect exclusive events with more than one photon. This domain is exclusive to shower detectors.

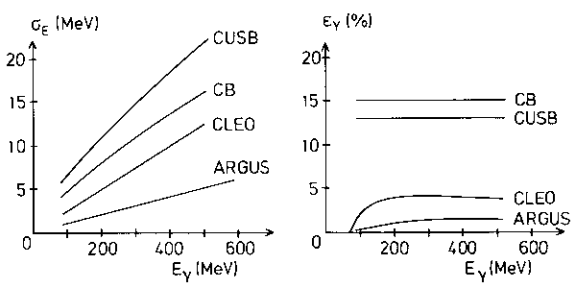

FIGURE 1
Sketch of the photon energy resolution functions and efficiencies relevant to the analysis of inclusive photons for all four detectors. Non-magnetic detectors detect photons in their shower counters, whereas magnetic detectors use e^+e^- pairs from converted photons.

Expectations for Radiative Decays from the $\Upsilon(1S)$

The only energetically allowed hadronic decay of the $\Upsilon(1S)$ requires the b and $\bar{b}$ quarks to annihilate into light hadrons at short distance. In QCD this process proceeds in lowest order through a three gluon intermediate state. This partial width is calculated[10] to be:

$$\Gamma(\Upsilon(1S) \to ggg) = \frac{160(\pi^2 - 9)}{81 M_\Upsilon^2}\, \alpha_s^3\, |\psi(0)|^2,$$

where α_s is the strong coupling constant, $\psi(0)$ is the $\Upsilon(1S)$ wave function at the origin, M_Υ the mass of the $\Upsilon(1S)$ resonance. In addition to this dominant decay mode a small fraction is expected to decay into a photon and two gluons. The ratio of these two partial rates, including first order QCD corrections,[11] is given by:

$$\frac{\Gamma(\Upsilon(1S) \to \gamma gg)}{\Gamma(\Upsilon(1S) \to ggg)} = \frac{36}{5}\,\frac{\alpha_{em}}{\alpha_s}\, q_b^2\, \left(1 + (2.2 \pm 0.6)\frac{\alpha_s}{\pi}\right),$$

where α_{em} is Sommerfeld's fine structure constant and q_b the bottom-quark charge. Evaluating this equation with[12] $\alpha_s = 0.2$ we obtain $\Gamma(\Upsilon(1S) \to \gamma gg)/\Gamma(\Upsilon(1S) \to ggg) \simeq 3\%$. Experimental results[13] confirm this expectation. Therefore we may expect some fraction of all $\Upsilon(1S)$ decays to proceed by emission of one photon and two gluons fragmenting into *one* resonance. The branching ratios for the radiative decays to ordinary $q\bar{q}$ mesons like $\pi^0, \eta, \eta', f(1270)$ have been calculated[14] to be less than about 2×10^{-4}. Experiments at the J/ψ indicate that particles like the ι and θ either contain a large gluon component or are manifestations of gluonium states predicted in QCD. For such gluon-gluon final states the branching ratios[15] are smaller than 1×10^{-6}. These predictions most likely put an observation from the $\Upsilon(1S)$ out of reach for current experiments.

A radiative $\Upsilon(1S)$ decay mode of very high interest leads to the production of the Higgs boson. This elusive particle is predicted in the Standard Model after spontaneous breakdown of the SU(2) symmetry group. As the theoretically lower limit[16] on the Higgs mass is about 7 GeV we can search for this particle in the mass region from $7\,\mathrm{GeV/c^2}$ up to the mass of the $\Upsilon(1S)$. The rate for this decay through the so-called Wilczek mechanism[17] is calculated to be:

$$\frac{\Gamma(\Upsilon(1S) \to \gamma + H)}{\Gamma(\Upsilon(1S) \to \mu^+\mu^-)} = \frac{G_F m_b^2}{\sqrt{2}\pi\alpha_{em}}\, \left(1 - \frac{M_H^2}{M_\Upsilon^2}\right),$$

where M_H is the mass of the Higgs, m_b the bottom quark mass, and G_F Fermi's weak coupling constant. Radiative QCD corrections and mixing effects with the P-wave bottonium states reduce this width further by a factor on the order of two.[18] The predicted branching ratio for a Higgs with a mass of e.g. $M_H = 8$ GeV is $B(\Upsilon(1S) \to \gamma H) \simeq 2 \times 10^{-5}$, too small to be detectable with current experiments. It has to be noted though, that in models with more

than one doublet of Higgs fields[19] this branching ratio could be substantially enhanced or suppressed.

Another possible rare decay mode of heavy quarkonium concerns the production of photinos and gluinos, which are the spin-half partners of photons and gluons in the framework of supersymmetric theories. Here we are mainly interested in the detection of a possible gluino-gluino bound state,[20] which, in the mass region under investigation, is predicted to have a total width of the order of 100 MeV for a $^1S_0$ state. The radiative branching ratio from the $\Upsilon(1S)$ depends strongly on the mass of the $(\tilde{g}\tilde{g})$ state; it can get as large as about 3×10^{-3} for masses of about 1 GeV. Again, for an assumed mass of $M_{\tilde{g}\tilde{g}} = 8$ GeV we may expect a branching ratio of $\simeq 3 \times 10^{-4}$. Although the total width is not as narrow as the photon energy resolution in a typical NaI detector, a detection in the inclusive photon spectrum seems feasible.

A very important task in $b\bar{b}$ physics experiments consists in measuring the hyperfine splitting. In principle this can be done by measuring the M1 transition $\Upsilon(1S) \to \gamma\eta_b$, where η_b is the $^1S_0$ state of bottonium. The predicted rate[21]

$$\Gamma(\Upsilon(1S) \to \gamma + \eta_b) = \frac{16}{3}\left(\frac{q_b}{2m_b}\right)^2 \alpha_{em}\, k^3\, |M_{if}|^2$$

is proportional to the third power of the radiated photon energy k. M_{if} is the overlap integral of the $\Upsilon(1S)$ and η_b wave functions: $M_{if} = \int r^2 \psi_i(r)\psi_f(r) j_0(kr/2) dr$ where j_0 is the spherical bessel function of order zero. As $j_0(kr/2 \ll 1) \simeq 1$ the matrix element is expected to be very close to 1 for allowed transitions between hyperfine partners with the same radial quantum numbers. Theoretical estimates for the mass splitting yield values between[22] 20 and[23] 100 MeV. Correspondingly, the branching ratios turn out to bracket values from about 1×10^{-5} to 1×10^{-3}. Current experimental sensitivity might be sufficient to test for mass-splittings between $\Upsilon(1S)$ and η_b down to about 100 MeV.

Experimental Results from the $\Upsilon(1S)$

During the summer of 1984 the Crystal Ball collaboration presented evidence[24] for a narrow state named $\varsigma(8.3)$ observed in the $\Upsilon(1S)$ inclusive photon spectrum. The branching ratio for this process was found to be

$$\mathrm{BR}(\Upsilon \to \gamma\varsigma) \times \mathrm{BR}(\varsigma \to \mathrm{hadrons}) = (0.5 \pm 0.1 \pm 0.3)\%.$$

The large systematic error is due to the uncertainty in modelling the decay mode of the ς. For this analysis it was assumed that the ς decays into a $c\bar{c}$ final state. Using a gg decay mode would reduce the branching ratio by about a factor of two. This ς signal was

substantiated by the observation of a second, less significant signal at the same mass using a statistically independent sample of $\Upsilon(1S)$ low multiplicity decays resembling the $\tau\tau$ channel. Both results came from a sample of about 100K $\Upsilon(1S)$ decays corresponding to a luminosity of $\mathcal{L} = 10.4 pb^{-1}$. The signal from the high (Fig. 2) and low multiplicity sample correspond to a combined significance of more than 5 s.d. if taken as independent manifestations of the same particle. Considerable excitement was caused by this finding and subsequently a large effort was undertaken to verify these initial findings. This was done both at CESR and DORIS. All four groups obtained luminosities exceeding the one in which evidence for the ζ was found. The number of resonance decays obtained are given in Table 2.

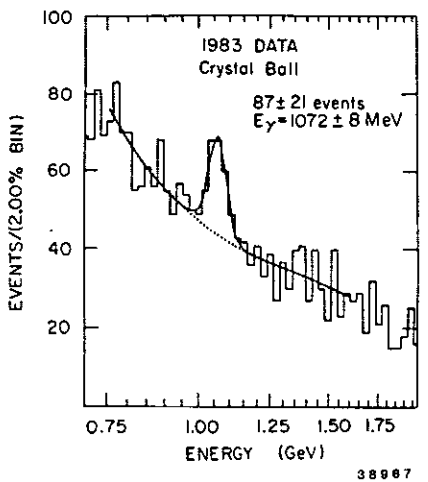

FIGURE 2
Results on $\Upsilon(1S) \rightarrow \gamma X$ inclusive photon spectrum from the Crystal Ball experiment. This shows the high multiplicity analysis as presented in the summer of 1984. The peak at 1.07 GeV was assigned to a resonance named ζ.

ARGUS	CLEO	CRYSTAL BALL	CUSB
200×10^3	260×10^3	200×10^3	400×10^3

TABLE 2
The total number of $\Upsilon(1S)$ resonance decays obtained by all four experiments since the announcement of the ζ in the summer of 1984.

Figs. 3 to 6 show the inclusive photon spectra obtained by all four experiments. No signal is apparent in any of the plots at a photon energy of about 1070 MeV corresponding to a transition to the ζ. The Crystal Ball collaboration has extensively checked their new data[25] (Fig. 3). In particular, energy calibration, energy resolution and multiplicities were

studied using known signals like inclusive π^0 and η invariant mass plots, the charged minimum ionizing peak at about 200 MeV, and the Bhabha peak. This study indicates that the ζ signal should again be found within ±1% of the old mass value and within ±5% of the width. The non-appearance of the ζ in the second data set is at present not understood by the Crystal Ball group and is still under study.

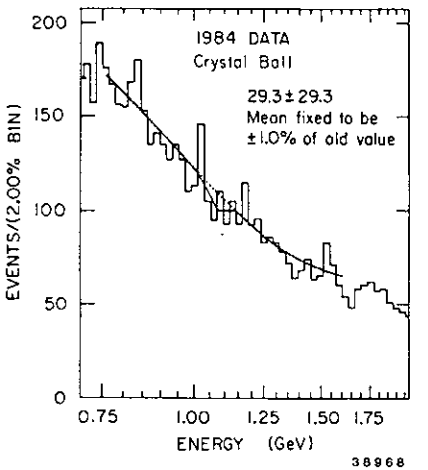

FIGURE 3
Results on $\Upsilon(1S) \rightarrow \gamma X$ inclusive photon spectrum from the Crystal Ball experiment. The plot is based on data accumulated in the summer of 1984. No peak is visible at the position of the ζ. The difference between this plot and Fig. 2 at the position of the ζ is more than 4 standard deviations.

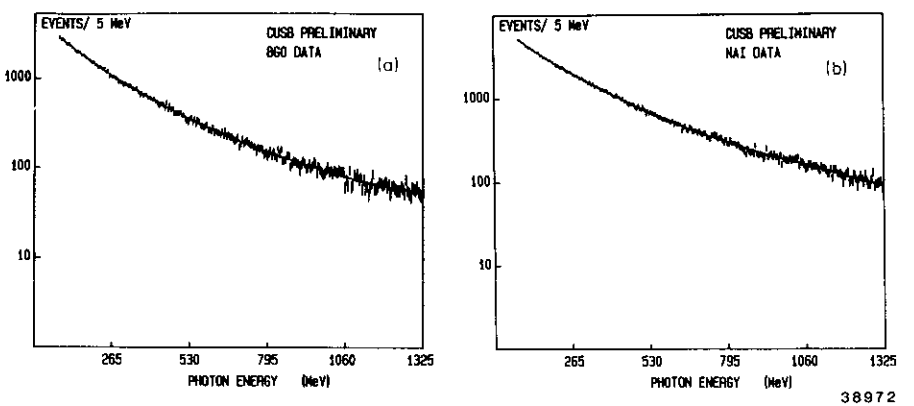

FIGURE 4
Results on $\Upsilon(1S) \rightarrow \gamma X$ inclusive photon spectrum from the CUSB experiment. These data were taken with a quadrant of BGO installed and are thus split into two parts. Photons detected in the BGO are shown in Fig. 4a (corresponding to 100K $\Upsilon(1S)$ decays), the analysis from the NaI detector is displayed in Fig. 4b (proportional to 300K $\Upsilon(1S)$ decays).

The CUSB results[26] displayed in Fig. 4 were obtained with a newly installed BGO quadrant. Therefore their inclusive photon spectrum is split into two parts containing photons measured in the NaI and in the BGO detector parts. No signal is found with a significance of more than 1 s.d. The model used to determine the efficiency to detect the final state is based on the process $\Upsilon \to \gamma gg$. The combined upper limit is calculated to be $BR(\Upsilon \to \gamma\varsigma) < 0.1\%$. Analyzing the inclusive photon spectra the CUSB group also sets an upper limit[28] of about 170 MeV on the mass-splitting between the $\Upsilon(1S)$ and the η_b. For a splitting of e.g. 100 MeV the upper limit is still a factor of 6 above the prediction, too far away to hope for any sign of the spin-singlet $^1S_0$ state.

Both magnetic detectors also studied the inclusive photon spectrum using converted photons in the beam pipe. CLEO increased the detection efficieny by including a 10% radiation length lead converter inside the drift chamber. Fig. 5 shows the spectrum obtained by CLEO[27]. The bin width used is roughly the FWHM of the resolution. The largest fluctuation, a 4 standard deviation effect at 520 MeV, is not considered a real effect due to missing confirmation by other experiments. At the position of the ς they obtain an upper limit of $BR(\Upsilon \to \gamma\varsigma) < 0.3\%$ compatible with the original ς branching ratio.

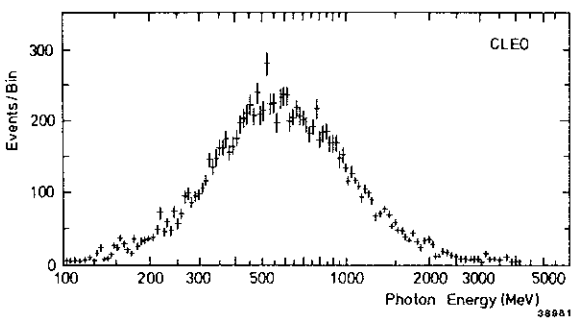

FIGURE 5
Results on $\Upsilon(1S) \to \gamma X$ inclusive photon spectrum from the CLEO experiment. A 10% radiation length lead converter was installed to enhance the photon detection efficiency. The bin width in this plot is about the FWHM of the resolution function for energies below 1 GeV.

ARGUS[28] has used not only converted photons to search for heavy mass resonances, but also studied photons in their shower counters. Therefore they obtain two independent results. Fig. 6a shows the spectrum as seen in the shower counters and Fig. 6b the one obtained using converted photons. Again no structure is visible over the whole spectrum. The combined upper limit is $BR(\Upsilon \to \gamma\varsigma) < 0.15\%$.

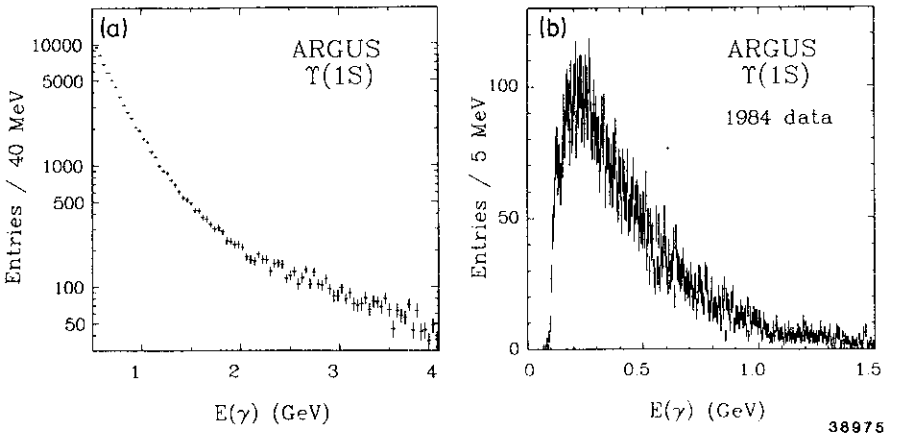

FIGURE 6
Results on $\Upsilon(1S) \to \gamma X$ inclusive photon spectrum from the ARGUS experiment. Fig. 6a shows the spectrum obseved with the barrel shower counters. The spectrum of photons converted in the beam-pipe or in the inner drift-chamber wall is diplayed in Fig. 6b.

One model which could possibly explain the disappearance of the ς is that of Tye and Rosenfeld.[29] Here the ς is viewed as a squark-antisquark $\tilde{q}\bar{\tilde{q}}$ resonance in its ground state. The ς is then produced by radiative decay of an excited $\tilde{q}\bar{\tilde{q}}$ state located near to the $\Upsilon(1S)$ resonance. Squarks here are not necessarily the supersymmetric partners of normal quarks; the only requirement is that squarks are scalar particles. A necessary prerequisite for this model requires that the two Crystal Ball data sets were obtained at (slightly) different beam energies. In particular, the second DORIS measurement should have been at the nominal $\Upsilon(1S)$ mass and the first one at a CMS value displaced by a small amount on the order of the CMS energy resolution of DORIS. This is confirmed by the average hadronic cross section as e.g. measured by the Crystal Ball experiment.[25] It indicates a possible shift in CMS energies of up to 8 MeV. The non-appearance in the second data set then implies[25] this squark-antisquark state to exist between about $16 - 26$ MeV above the $\Upsilon(1S)$. The experiments at CESR might not have been in a position to excite such a state due to CESR's superior energy resolution. It has to be noted though, that the ad hoc nature of the assumptions render this explanation rather unlikely. Given the negative results obtained by ARGUS, CUSB and the second run of the Crystal Ball, the existence of the ς seems very unlikely.

All groups have derived upper limits[25-28] for the branching ratio $BR(\Upsilon \to \gamma + X)$ where X is any narrow state. To illustrate the strength of those limits we present the determination by the CUSB group as their analysis is based on the largest data sample. Fig. 7 shows the 90% confidence level upper limit plotted versus the mass-squared of a particle recoiling against the

radiated photon. Also in Fig. 7 is plotted the theoretical expectation (dashed curve) in lowest order[17] for a light neutral Higgs boson. Including QCD radiative corrections and mixing effects[18] such a particle is ruled out up to masses of about 2 GeV. As has been stated above, the theoretical lower limit on the mass for the Higgs in the standard one-doublet model is[16] about 7 GeV, but is completely unconstrained in models with more than one doublet.

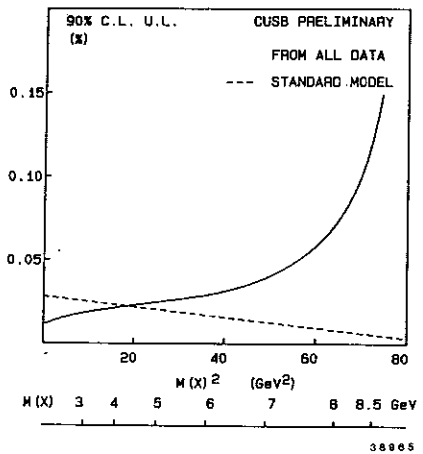

FIGURE 7
CUSB result on the 90% upper limit for the branching ratio BR($\Upsilon \to \gamma + X$) (solid line) where X is any narrow state. Data from the BGO and NaI parts of the detector have been added to obtain the upper limit. Also shown (dashed line) is the prediction for the production of a Higgs in the one-doublet minimal standard model.

Summarizing we note that none of the exciting $\Upsilon(1S)$ radiative decay modes in the Standard Model have shown up yet. This is expected due to the rather small branching ratios predicted. No extension of the Standard Model is required by experiment. The ς seemed like a nice candidate for several theories but its existence seems now very unlikely. The $^1S_0$ state has not yet been seen, and it is expected that significantly more data are needed to allow its discovery.

POTENTIAL MODELS

At the present time, QCD processes can be evaluated only as a perturbation series expansion. The first few terms of this expansion should provide a good approximation as long as the expansion parameter $\alpha_s(Q^2)$ is small, which happens when Q^2 is large. However, many interesting questions about hadrons belong to the regime of small Q^2, where the perturbation series breaks down. To describe for example the static properties of hadrons it is therefore appropriate to use models. These models could either be inspired by QCD or be purely phenomenological.

Heavy quarkonia provide direct evidence for the quark structure of hadrons. As the strongly interacting constituents are heavy, relativistic effects are small and a sufficiently accurate approximation is obtained by a non-relativistic treatment. It is based on the Schrödinger equation with a static potential $V_{n.r.}$

$$\left[-\frac{1}{m_b}\nabla^2 + V_{n.r.}(r)\right]\psi(r) = E\,\psi(r).$$

The main problem consists in choosing the correct non-relativistic potential and determining the free parameters of the potential by a fit to the data. So far the potential cannot be computed in QCD from first principles and we have to rely on models. However, numerical studies of the interquark potential have been started[30] using the lattice gauge theories of QCD. The results obtained are in good agreement with the potential models discussed below.

Given the nearly equal splittings between the 2^3S_1 and the 1^3S_1 in charmonium and bottonium it has been suggested to use a purely phenomenological potential with a logarithmic form[31] $V(r) = C\ln(r/r_0)$ or with a power potential[32] $V(r) = A + Br^\epsilon$. The latter ansatz reduces to a logarithmic form for small ϵ. The value obtained from the fits turns out to be small, $\epsilon \simeq 0.1$. Both of these models are quite successful and they will also be used later on for comparison with experimental data.

One of the first attempts[21] to fit the heavy J/ψ mass spectrum used a potential of the form $V_{n.r.} = -\frac{4}{3}\frac{\alpha_s}{r} + kr$. This form is suggested by lowest order QCD. The Coulomb-like form arises from one gluon exchange between quarks and dominates at short distances. At large distances the linear part is important. It is motivated by the string (a chromo-electric tube) picture of quark confinement. In later work[33] the short-distance Coulomb and the long-distance linear potentials were connected logarithmically at intermediate distances.

The QCD inspired potentials discussed so far do not incorporate asymptotic freedom. This can be achieved by either softening the r-dependance[34] of the Coulomb-like term or by establishing the potential in momentum space making e.g. direct use of the results of the QCD β-function. A particularly simple and successful example with the latter approach was suggested by Richardson[35]

$$V(q^2) = -\frac{4}{3}\,\frac{12\pi}{33-2n_f}\,\frac{1}{q^2\ln\left(q^2/\Lambda^2+1\right)}$$

which depends only on a single scale parameter Λ as it should be the case for a true QCD potential. Note that this parameter can be related[36] directly to the scale parameter $\Lambda_{\overline{MS}}$ in the QCD minimal subtraction scheme. Most of the models to be used below for comparison with experimental data are based on this ansatz in momentum space. Although the procedure of constructing a potential is not unique, all approaches lead to very similar potential forms in the region of distances under study from about 0.1 to 1.0 fm, see Fig. 8. The models

begin to differ substantially for inter-quark separations less than about 0.1 fm. Therefore, as long as the expected very heavy quark $t\bar{t}$ system is not observed, we have to search for effects which probe the very short distance region. In order to verify that QCD really governs the interaction between quarks, tests are needed which distinguish the QCD from the purely phenomenological approach. One such probe is the fine and hyper-fine splitting of bottonium.

Unfortunately, theoretical calculations are not free of problems. All potential models are in some sense phenomenological as they have not been strictly derived from QCD. An exception are lattice gauge theories which, in the near future, will yield quantitative predictions for heavy quark systems.[30] Currently, QCD corrections for the potential and decays of heavy quarkonia can only been calculated in next-to-leading order. Due to the large size of the strong coupling constant α_s these corrections are not always small enough to give confidence in a rapid convergence of the expansion series. As a result QCD predictions often have an error of 20% or more even in the perturbative regime. Another problem concerns the correct choice of the QCD scale at which to evaluate the running coupling constant α_s. This choice[12] seems to depend more on personal intuition than on stringent physics requirements. Finally, a fully relativistic treatment has only been done for the spin-0 Klein-Gordon equation;[37] so far relativistic corrections were incorporated into the hamiltonian up to order $(v/c)^2$. Today, all these problems are under close investigation.

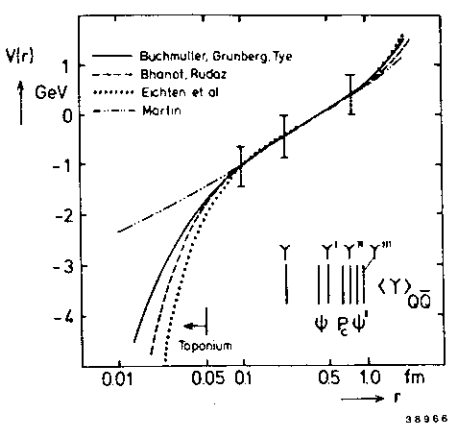

FIGURE 8
The radial dependence of some typical quark-antiquark potentials for heavy quarkonia systems (from Ref. 36). The potentials have been shifted to agree at a radius of $r = 0.5$ fm. The average radii $(\sqrt{< r^2 >})$ of the observed $c\bar{c}$ and $b\bar{b}$ states are indicated. The potential models used are by Bhanot and Rudaz (Ref. 33), Buchmüller, Grunberg and Tye (Ref. 36), Eichten *et al.* (Ref. 21) and Martin (Ref. 32).

Spin-dependent mass-splittings –an intrinsically relativistic effect – are incorporated into the non-relativistic treatment by means of the Bethe-Salpeter and Breit-Fermi equations, where the latter is the most popular approach. The method chosen is analogous to the QED

analysis of positronium. The general result[38] is given by

$$V_{spin}(r) = \frac{1}{2m_b^2}(\vec{L}\cdot\vec{S})\frac{1}{r}\left(V'_{n.r.} + 2V'_1 + 2V'_2\right) - \frac{1}{3m_b^2}\left(3(\vec{S_1}\cdot\hat{r})(\vec{S_2}\cdot\hat{r}) - \vec{S_1}\cdot\vec{S_2}\right)V_3 + \frac{1}{3m_b^2}\left(\vec{S_1}\cdot\vec{S_2}\right)V_4\,,$$

where the prime denotes differentiation with respect to the radial coordinate r. The three terms are the spin-orbit, the tensor and the spin-spin interaction potentials, respectively. The ${}^3P_J$ states, which have orbital angular momentum $L = 1$ and total spin $S = 1$, are split by the spin-orbit and tensor forces only. The spin-dependent potentials V_i obey the important equation[39] $V_1(r) - V_2(r) + V_{n.r.}(r) = 0$. Together with this relation the properties of the confining and Coulomb potentials under Lorentz transformations can be determined. The Coulomb-like potential arises from the exchange of a vector particle, the gluon, and therefore transforms like a Lorentz-vector (V_v). The confining part is required to be purely scalar (V_s). With $V_{n.r.} = V_v + V_s$, $V_2 = V_v$, and V_3, V_4 given in analogy to QED we obtain:[39]

$$V_{spin}(r) = \frac{1}{2m_b^2}(\vec{L}\cdot\vec{S})\left(\frac{3V'_v - V'_s}{r}\right) - \frac{1}{3m_b^2}\left(3(\vec{S_1}\cdot\hat{r})(\vec{S_2}\cdot\hat{r}) - \vec{S_1}\cdot\vec{S_2}\right)\left(V''_v - \frac{V'_v}{r}\right) + \frac{2}{3m_b^2}\left(\vec{S_1}\cdot\vec{S_2}\right)\nabla^2 V_v\,.$$

For comparison with experimental mass splittings we need to take the expectation value of this spin-dependent potential. We introduce obvious abbreviations a, b, c and write the general spin-dependent energies

$$\langle V_{spin}(r)\rangle = a\,\langle\vec{L}\cdot\vec{S}\rangle + b\,\langle 3(\vec{S_1}\cdot\hat{r})(\vec{S_2}\cdot\hat{r}) - \vec{S_1}\cdot\vec{S_2}\rangle + c\,\langle\vec{S_1}\cdot\vec{S_2}\rangle \quad \text{with}$$

$$a = \frac{1}{2m_b^2}\langle\frac{3V'_v - V'_s}{r}\rangle; \quad b = \frac{-1}{3m_b^2}\langle V''_v - \frac{V'_v}{r}\rangle; \quad c = \frac{2}{3m_b^2}\langle\nabla^2 V_v\rangle\,.$$

In the case of the ${}^3P_J$ states the hyperfine term $\vec{S_1}\cdot\vec{S_2}$ does not contribute to the mass-splitting and we need only evalute the matrix elements of $\vec{L}\cdot\vec{S}$ and the tensor term (see *e.g.* Ref. 40):

$$\langle V_{{}^3P_J}\rangle = \frac{1}{2m_b^2}\langle\frac{3V'_v - V'_s}{r}\rangle\begin{Bmatrix}-2\\-1\\+1\end{Bmatrix} + \frac{-1}{3m_b^2}\langle V''_v - \frac{V'_v}{r}\rangle\begin{Bmatrix}-1\\+1/2\\-1/10\end{Bmatrix} \quad \text{for } J = \begin{Bmatrix}0\\1\\2\end{Bmatrix}.$$

With the help of these expectation values and the mass values from experiment we can derive the parameters a and b und thus gain information on the potentials. As b is proportional to derivatives of the vector (Coulomb) potential, it yields direct information on the short-range behaviour of the force acting between two quarks. The a term is proportional to the expectation value of both the vector (Coulomb) and scalar (linear) potentials. It may therefore yield information on the confining part of the potential.

Of great interest would be the discovery of the $^1P_1$ state. Its mass, compared to the center-of-gravity of the ^3P_J states, reveals the hyperfine part of the spin force. As shown above this part is a contact term ($\nabla^2 V_v$) and thus would give information on the very short range part of the potential accessible otherwise only with a much heavier quarkonium system.

How do we obtain information on the fine-splitting in the bottonium system? The easiest way consists of searching for the radiative transitions from the $^3S_1$ to the ^3P_J states. The rate for these electric dipole transitions is given by[21]

$$\Gamma(\Upsilon(2S) \to \gamma + {}^3P_J) = \frac{4}{27}(2J+1)\, q_b^2\, \alpha_{em}\, k^3\, |E_{if}|^2 ,$$

where E_{if} is the transition dipole matrix element involving the overlap integral of the $^3S_1$ and ^3P_J wave functions. Due to the sensitivity to details of the wave function, in particular the position of the nodes, predictions are most reliable for non-relativistic systems like bottonium. We therefore may expect good agreement between data and theory. As mentioned in the section on $\Upsilon(1S)$ radiative decays, current experimental sensitivity is not yet sufficient to detect the $^1S_0$ state of bottonium.

Radiative Decays from the $\Upsilon(2S)$

All four experiments have obtained results on the radiative transitions $\Upsilon(2S) \to \gamma + {}^3P_J$. This can be done in two ways, either by studying the inclusive photon spectrum in hadronic events or by analyzing the fully exclusive decay chain. In the latter case the ^3P_J is required to decay radiatively to the $\Upsilon(1S)$, which is detected in its known leptonic decay modes: $\Upsilon(2S) \to \gamma + {}^3P_J \to \gamma\gamma\Upsilon(1S) \to \gamma\gamma\ell^+\ell^-$. As mentioned above, only the non-magnetic detectors are in a position to study this exclusive reaction.

The first results on the ^3P_J states came from the CUSB[41] detector (Fig. 9) and later from CLEO.[42] Note that CLEO has re-analyzed their data[27]; Fig. 10 shows their latest spectrum. Both experiments agree nicely on the position of the two lowest photon energies at about 108 MeV and 128 MeV, which, in analogy with the charmonium system where the ^3P_J spins have been measured, are assumed to correspond to the states with spin $J = 2$ and 1. The agreement for the third line is not so good. CUSB determined the line at

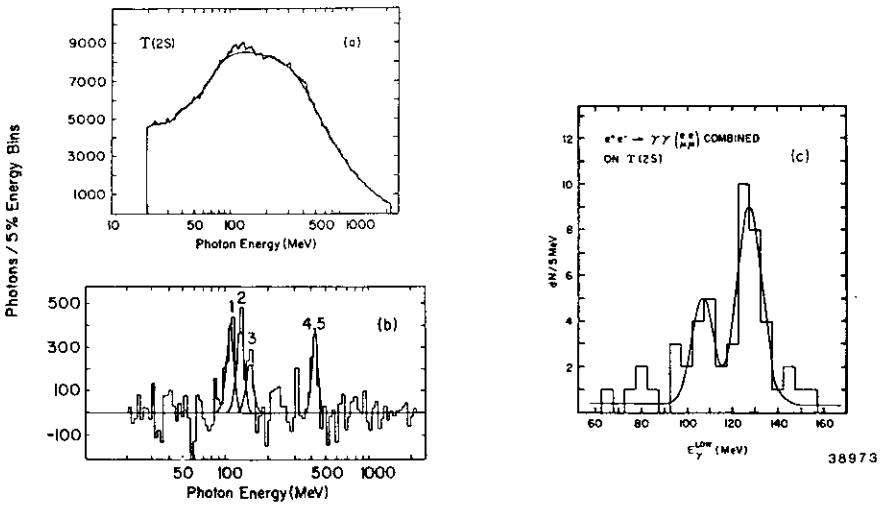

FIGURE 9
Results on $\Upsilon(2S) \to \gamma X$ decays from the CUSB experiment. Fig. 9a shows the inclusive photon spectrum. The background subtracted spectrum (Fig. 9b) is fit with four Gaussians, three for the initial photon lines to the ^3P_J and one for the secondary transitions. The result on the exclusive decays after a constraint fit is displayed in Fig. 9b.

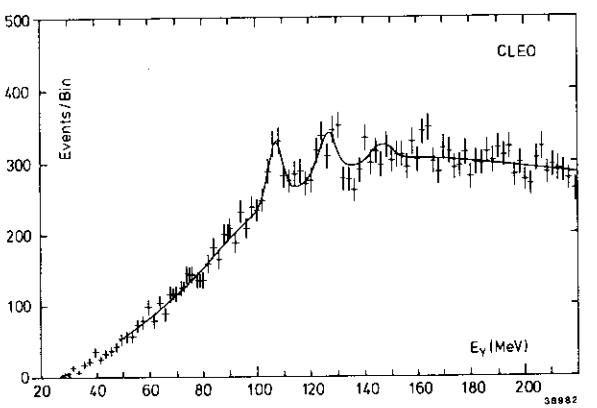

FIGURE 10
Results on $\Upsilon(2S) \to \gamma X$ decays from the CLEO experiment using e^+e^- pairs from converted photons. The spectrum is from a re-analysis[27] performed this year. The bump at 149 MeV in the fit is forced to coincide in energy and branching ratio with the corresponding CUSB measurement. The fit prefers a photon energy of 165 MeV.

about 149 MeV. In contrast, CLEO found it around 160 MeV, but with less than 2 standard deviation significance. The bump in CLEO's spectrum (Fig. 10) at 149 MeV is forced in energy and branching ratio to coincide with CUSB's measurement. Clearly the data are inconsistent with these assumptions. Due to the (expected) rather small branching ratio for the secondary transition from the $^3P_0$ to the $\Upsilon(1S)$, the analysis of the exclusive final state cannot shed light on this problem. More experiments were needed to resolve this discrepancy.

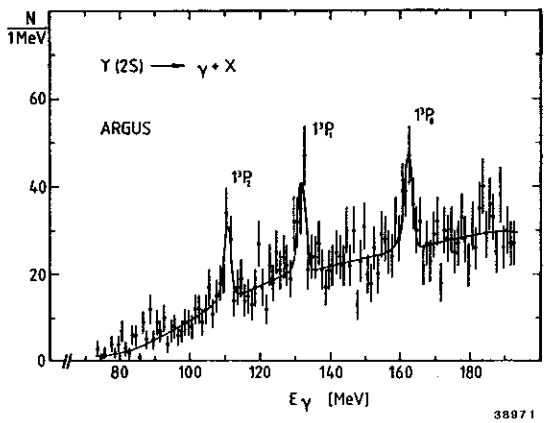

FIGURE 11
Results on $\Upsilon(2S) \rightarrow \gamma X$ decays from the ARGUS experiment. The curve shows the best fit to three photon lines with a shape given by the detector resolution for converted photons. Note the very good resolution of about $\sigma_E \simeq 1.1$ MeV.

By the summer of 1984 both detectors at DORIS had accumulated enough statistics to search for these transitions. Figs. 11 and 12 show the results obtained by the ARGUS[43] and Crystal Ball[44] collaborations. Both experiments confirm the original CESR measurements on the two lowest energetic photon transitions. The highest energy line is firmly established with high statistical significance at about 162 MeV. Table 3 collects all the results on photon energies and branching ratios. A plot of these measurements is depicted in Fig. 13. The energies obtained in inclusive and exclusive reactions by the non-magnetic detectors have been averaged using weighted means. Statistical and systematic errors have also been combined in quadrature to allow an easier comparison. The last row shows the average of all measurements. The CLEO values on the third line are omitted from the averages as this line is not unambigously implied by their data. Although the CUSB highest energy line disagrees with the other experiments, the average energy and branching ratio change very little (within the errors) when the CUSB values are excluded. This is due to the very accurate photon energy determination from ARGUS and the similarity in all branching ratios for the third line.

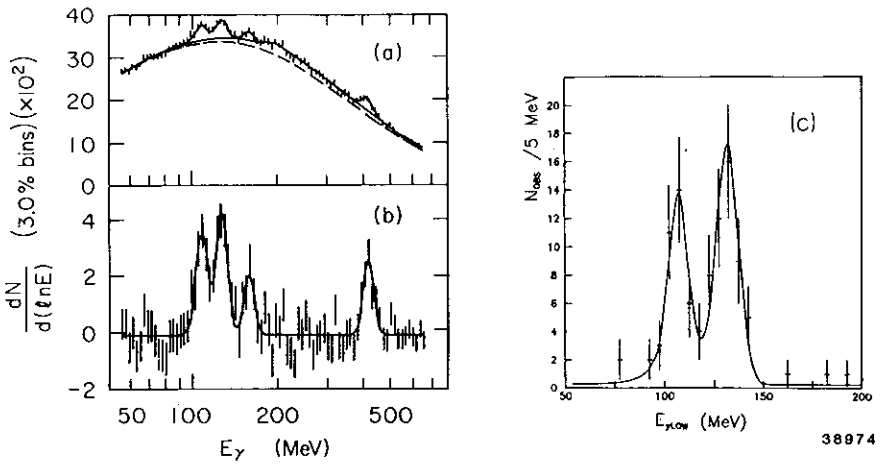

FIGURE 12
Results on $\Upsilon(2S) \rightarrow \gamma X$ decays from the Crystal Ball experiment. Fig. 12a shows the inclusive photon energy spectrum. The background subtracted spectrum is shown in Fig. 12b. The primary transitions to the ^3P_J states between 100 and 160 MeV and the overlap of the secondary transitions from those states down to the $\Upsilon(1S)$ are apparent. The result of the fully exclusive analysis is shown in Fig. 12c. The two primary transitions are nearly completely seperated. A similar spectrum is used to determine the spins of the ^3P_J.

Although all experiments agree on the energies of the two lowest transitions, the branching ratios differ by more than 1 standard deviation. The magnetic detectors seem to measure higher values than the non-magnetic detectors. This may be due to the difficulty for magnetic detectors to determine the photon efficiency at the very low energetic end where electrons from converted photons curl-up and track-finding algorithm are less efficient (see Fig. 1). Non-magnetic detectors on the other hand provide a constant efficiency over the whole energy range. Using the displayed average values on the energies we calculate the world-average of the ^3P_J masses. Table 4 gives the result. With these values the spin weighted average of the P-states, the center-of-gravity (COG), defined by $M_{P_{cog}} = \frac{1}{9}(\sum(2J+1)M_J)$, yields $M_{P_{cog}} = 9900.6 \pm 0.6$ MeV.

The angular distributions of the photons emitted in the decay of the $\Upsilon(1S)$ and the ^3P_J depend on the spin J of the latter state. The large background under the photon lines in the inclusive analyses prohibit a spin determination. The exclusively measured decays, however, have very little background contribution; see Fig. 9 and Fig. 12. Due to the very good energy resolution of the Crystal Ball NaI detector the two low-energy monochromatic photon lines

Experiment	Photon Energy (MeV)	Branching Ratio (%)
ARGUS	110.6 ± 0.9	9.8 ± 3.2
	131.7 ± 1.1	9.1 ± 2.8
	162.1 ± 1.5	6.4 ± 2.1
CLEO	109.0 ± 0.7	11.4 ± 2.1
	128.6 ± 1.0	7.8 ± 1.9
	(165.1 ± 2.8)	(3.0 ± 1.8)
CRYSTAL BALL	108.2 ± 1.6	5.8 ± 1.2
	131.4 ± 1.5	6.5 ± 1.4
	163.8 ± 3.1	3.6 ± 1.2
CUSB	107.7 ± 1.5	6.1 ± 1.4
	128.0 ± 1.3	5.9 ± 1.4
	149.4 ± 5.0	3.5 ± 1.4
Average	109.3 ± 0.5	7.0 ± 0.8
	130.0 ± 0.6	6.8 ± 0.8
	161.6 ± 1.3	4.0 ± 0.8

TABLE 3
Photon energies and branching ratios measured by the four experiments. Note that the results on the photon energies from the non-magnetic detectors are an average of their inclusive and exclusive results. Weighted means are used to calculate the overall world averages. The measurements by CLEO on the highest energy line are not included in the average, as their data do not unambigously imply this state.

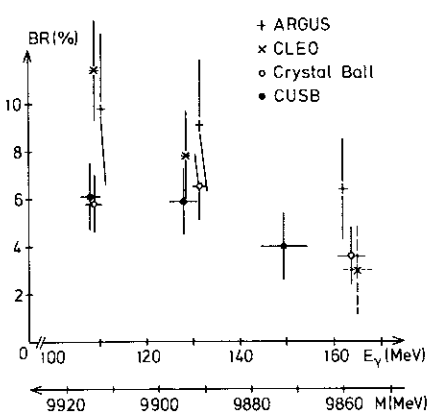

FIGURE 13
Results on $\Upsilon(2S) \rightarrow \gamma^3P_J$ decays from all four experiments. Plotted is the branching ratio versus the photon energy. Where appropriate, inclusive and exclusive measurements have been averaged using weighted means. Systematic and statistical errors are added in quadrature.

are resolved (Fig. 12). The feeddown from one line into the other and additional background is less than 12%. Unfortunately the total number of events for each decay chain is only about 70. Such a small data set does not allow a model-independent determination of the spin. But according to the quarkonium model only three possible spin values need to be considered for ^3P_J states: $J = 0, 1$ and 2. This fact is used in the analysis.[45] In addition, the multipolarity of the photon transitions are assumed to be purely dipole.

Using the logarithmic likelihood a test function for definite spin is defined in terms of the theoretical angular correlation function.[46] In a first step both lines are tested for a spin 0 assignment. The confidence level for this hypothesis is smaller than 0.2%. In a second step a combined test on both lines is performed under the hypothesis that one of the states has spin 2 and the other one has spin 1. The confidence level for spin values opposite to expectation is again smaller than 0.6%. This observation effectively determines the spin assignments as given in Table 4.

State	$^3P_0$	$^3P_1$	$^3P_2$
MASS (MeV)	9860.5 ± 1.3	9892.6 ± 0.7	9913.5 ± 0.6

TABLE 4
The world-average values for the masses of the ^3P_J states in bottonium. The photon-energies from all four experiments are included in the average. The mass of the $\Upsilon(2S)$ obtained by several depolarisation experiments is taken from Ref. 47. The center-of-gravity is calculated with these mass-values to $M_{P_{cog}} = 9900.6 \pm 0.6$ MeV.

Supporting evidence comes from an analysis of the branching ratios $\Upsilon(2S) \rightarrow \gamma + ^3P_J$. As shown in the last section, the rates for these processes are related to the spin of the ^3P_J and to the third power of the radiated photon energy: $\Gamma \propto (2J+1)\,k^3$; the dipole maxtrix element should be the same for all three cases. Dividing the experimental branching ratios by the factor $(2J+1)\,k^3$ and the branching ratio of the second line, we obtain for the expected spin assignments a ratio of $(0.9 \pm 0.2 : 1 : 1.0 \pm 0.2)$, in agreement with the theoretical ratio of reduced widths $1 : 1 : 1$. Any other spin combination yields significantly different ratios.

COMPARISON WITH THEORY

As discussed above the averaged spin-dependent part of the potential can be written

$$\langle V_{spin}(r) \rangle = a\,\langle \vec{L} \cdot \vec{S} \rangle + b\,\langle T_{12} \rangle + c\,\langle \vec{S_1} \cdot \vec{S_2} \rangle$$

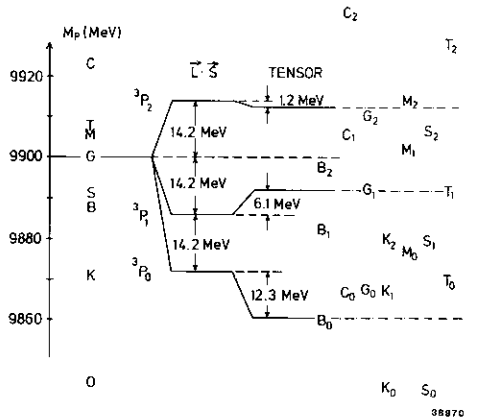

FIGURE 14
Indicated is the splitting of the ^3P_J states from the center-of-gravity (COG) due to the relativistic spin-orbit and tensor forces. The mass splittings are obtained using the world-average of the ^3P_J masses (see Table 4). In addition, predictions are shown from some potential-models for the COG and the individual spin-triplet masses. The following abbreviations are used: B = Buchmüller, Ref. 49; C = McClary and Byers, Ref. 23; G = Gupta *et al.*, Ref. 48; K = Khare, Ref. 50; M = Moxhay and Rosner, Ref. 51; O = Grotch *et al.*, Ref. 52; S = Bander *et al.*, Ref. 53; T = Ono and Törnqvist, Ref. 54.

where the last term, the hyperfine part, is constant for the ^3P_J states under consideration. It is also customary to define a ratio $r = (M_2 - M_1)/(M_1 - M_0)$ where M_J are the masses for the states with total spin J. In terms of a and b this ratio is given by $r = (2a - 0.6b)/(a + 1.5b)$. We feel that, given the accuracy of today's world average value for the P-masses it is more appropriate to study the individual parameters a and b instead of the ratio r. This way the full information is kept for a deeper understanding.

With the above given world-averaged ^3P_J masses we obtain the following values for the parameters a and b:

$$a = \frac{1}{2m_b^2}\left(\frac{3V_v' - V_s'}{r}\right) = 14.1 \pm 0.4 \text{ MeV}$$

$$b = \frac{-1}{3m_b^2}\left(V_v'' - \frac{V_v'}{r}\right) = 12.0 \pm 0.9 \text{ MeV}.$$

For comparison with theory the corresponding values of the expectation parameters are included in Table 5. Also given are the values determined for the $c\bar{c}$ system and the $2\,^3P_J$ $b\bar{b}$ states. The mass values used are from the Particle Data Group[47] and from Ref. 26. The model by Gupta *et al.*[48] which includes higher order QCD corrections is in excellent agreement with the data. Also the model by Grotch *et al.*[52] predicts a and b rather accurately but fails in the prediction for the center-of-gravity.

If we were to set the long-range potential to zero we would retain the spin dependence as in pure QED. With the standard Coulomb force this yields the relation $a = 1.5b$ (QED). The experimental values in Table 5 indicate that the heavy $b\bar{b}$ system is close to this value. For the $c\bar{c}$ system the relation $a < b$ reveals the importance of the long-range component of the force. This can most easily be seen by evaluating the expectation values with the standard potentials $V_v = -4\alpha_s/3r$ and $V_s = kr$. We obtain $a = 1.5b - \frac{1}{2m^2}\langle k/r\rangle$. It is therefore quite reasonable to assume that the parameters a and b from the ^3P_J indicate the approach of the spin dependent potentials to their perturbative form.

ORIGIN	a (MeV)	b (MeV)	r
$1\,^3P_J$ $(b\bar{b})$ (Expt.)	14.1 ± 0.4	12.0 ± 0.9	0.65 ± 0.05
Buchmüller *et al.*, Ref. 49	10.3	7.7	0.73
McClary *et al.*, Ref. 23	17.3	21.1	0.45
Gupta *et al.*, Ref. 48	11.3	9.1	0.68
Khare, Ref. 50	9.0	10.0	0.50
Moxhay *et al.*, Ref. 51	8.9	11.3	0.42
Grotch *et al.*, Ref. 52	14.0	10.0	0.76
Bander *et al.*, Ref. 53	17.1	11.9	0.77
Ono *et al.*, Ref. 54	12.0	6.7	0.91
$2\,^3P_J$ $(b\bar{b})$ (Expt.)	10.3 ± 1.2	8.2 ± 3.3	0.70 ± 0.23
$1\,^3P_J$ $(c\bar{c})$ (Expt.)	34.9 ± 0.3	40.1 ± 0.8	0.48 ± 0.01

TABLE 5
Expectation values of the spin-orbit (a) and tensor (b) potentials as determined from the experimental and theoretical ^3P_J masses. Included are also the corresponding values for the charmonium system[47] and the $2\,^3P_J$ of bottonium[26] for comparison. The ratio r is defined in the text.

Using the expectation values as determined from experiment we find that the state with spin $J = 0$ is shifted downward from the center-of-gravity by about 28 MeV due to the $\vec{L}\cdot\vec{S}$ term and by another 12 MeV due to the tensor term. On the other hand, the state with spin $J = 2$ is mostly affected by the $\vec{L}\cdot\vec{S}$ term and shifted upward by about 13 MeV. See Fig. 14 for a sketch of the influence of the spin-orbit and tensor forces on the P states. Also indicated in Fig. 14 are the predictions from several potential models. As stated above, the prediction by Gupta *et al.*[48] reproduces the experimental results best, but also some earlier models do not fare badly, although some miss the COG substantially. This is due to an over/under - estimate of the long-range force component and not of the spin splittings. It has to be noted though, that the purely phenomenological model by Khare,[50] based on Martin's[52]

original approach, reproduces neither the COG nor the splittings correctly. This fact can be viewed as a success for the potentials based on QCD. They seem to have the right ingredients like one-gluon exchange, asymptotic freedom and linear confinement. Therefore these models should in principle allow a determination of the only scale-parameter in QCD, $\Lambda_{\overline{MS}}$.

Indeed Buchmüller *et al.*[36] have found a lower bound on the scale parameter of QCD, $\Lambda_{\overline{MS}} > 100$ MeV, from an analysis of the charmonium and bottonium data. Recently, Hagiwara *et al.* have re-analysed[55] these data including both the $1P$ and $2P$ measurements. Of course they could not include the final masses discussed here and doing so should improve their results significantly. They obtain $\Lambda_{\overline{MS}} = 250 \pm 100$ MeV, a value equal to that obtained by an analysis of all processes which measure the running coupling constant of QCD.[12] Their study also shows that the observation of the expected $t\bar{t}$ system would not increase significantly the precision on the QCD scale parameter. Therefore an important approach to a more accurate determination of $\Lambda_{\overline{MS}}$ seems a precision study of the bottonium system. In particular we need more precise masses of the $2\,^3P_J$ states and more precise leptonic widths of all $^3S_1$ states. Given the relative ease of experimentation at the Υ (over a $t\bar{t}$) system this route seems to offer many prerequisites for a detailed understanding of QCD and it's scale parameter.

Hadronic Width of ^3P_J States

As has been mentioned above, both non-magnetic detectors have measured the fully exclusive decay chain $\Upsilon(2S) \to \gamma + {}^3P_J \to \gamma\gamma\Upsilon(1S) \to \gamma\gamma\ell^+\ell^-$ and obtain the branching ratios listed in Table 6. With the inclusive branching ratios given in Table 3, the branching ratios for the decay of the ^3P_J states can be calculated to

$$\begin{aligned} \mathrm{BR}(^3P_0 \to \gamma\Upsilon(1S)) &< 6\% \\ \mathrm{BR}(^3P_1 \to \gamma\Upsilon(1S)) &= (29 \pm 6)\% \\ \mathrm{BR}(^3P_2 \to \gamma\Upsilon(1S)) &= (21 \pm 5)\%. \end{aligned}$$

Each radiative branching ratio can be converted into a hadronic width for these states with $\Gamma_{had} = \Gamma_\gamma(\frac{1}{\mathrm{BR}_\gamma} - 1)$ if we use some estimate for the E1 width Γ_γ. It turns out that in potential models the prediction for this radiative width is rather stable, especially for the $b\bar{b}$ system. This is demonstrated nicely in Ref. 23. To further justify the use of theoretical input for Γ_γ, we compare the E1-widths for the transitions from the $\Upsilon(2S)$ to the P-states. The results are given in Table 7. The agreement between data and prediction is satisfactory. The differences between different models are due to relativistic corrections which, for the $b\bar{b}$ system under consideration, are on the order of 10%.

Experiment	BR($^3P_0$) (%)	BR($^3P_1$) (%)	BR($^3P_2$) (%)
Crystal Ball	< 0.2	2.1 ± 0.4	1.6 ± 0.4
CUSB	< 0.4	1.9 ± 0.4	1.3 ± 0.4
Average	< 0.2	2.0 ± 0.3	1.5 ± 0.3

Table 6
Branching ratios for the fully exclusive decay chain with the leptonic BR $\Upsilon(1S) \to \gamma\gamma\ell^+\ell^-$ divided out. The notation is: $\mathrm{BR}(^3P_J) = \mathrm{BR}(\Upsilon(2S) \to \gamma + {}^3P_J \to \gamma\gamma\Upsilon(1S))$. Experimental values are from Refs. 26 and 44. Systematic and statistical errors are added quadratically. The last row shows the average BRs obtained by taking the weighted means of the individual results. The upper limits on the $^3P_0$ branching ratios are at the 90% confidence level.

Width (keV)	$\Gamma(\Upsilon' \to \gamma^3P_0)$	$\Gamma(\Upsilon' \to \gamma^3P_1)$	$\Gamma(\Upsilon' \to \gamma^3P_2)$
Experiment, see Table 3	$1.2 \pm 0.2 \pm 0.2$	$2.0 \pm 0.2 \pm 0.3$	$2.1 \pm 0.2 \pm 0.3$
Buchmüller *et al.*, Ref. 49	1.5	2.3	2.3
McClary *et al.*, Ref. 23	1.0	1.9	2.2
Grotch *et al.*, Ref. 52	1.1	2.3	2.6
Gupta *et al.*, Ref. 48	1.4	2.2	2.2
Moxhay *et al.*, Ref. 51	1.5	2.9	2.5

Table 7
The Γ_γ widths for the radiative transitions from the $\Upsilon(2S)$ to the ^3P_J states. The experimental values are determined using the average branching ratios from Table 3 and the total width of the $\Upsilon(2S)$ from Ref. 47. The first error is the total error on the branching ratio, the second error reflects the uncertainty in the $\Upsilon(2S)$ total width, $\Gamma_{tot} = 29.6 \pm 4.7$ keV. The theoretical values from the cited references are adjusted for measured photon energies.

The secondary transitions from the P-states to the $\Upsilon(1S)$ are affected very little by relativistic corrections as the overlap integral is insensitive to the detailed form of the wave functions.[23] To obtain $\Gamma_\gamma(^3P_J \to \gamma\Upsilon(1S))$ we use recent QCD-type potential models (Refs. 48, 49, 51, 52, 53) which predict the COG and splittings of the P-states adequately. We find

$$\begin{aligned} \Gamma(^3P_0 \to \gamma\Upsilon(1S)) &= 27\ (\pm 3)\,\mathrm{keV} \\ \Gamma(^3P_1 \to \gamma\Upsilon(1S)) &= 33\ (\pm 3)\,\mathrm{keV} \\ \Gamma(^3P_2 \to \gamma\Upsilon(1S)) &= 39\ (\pm 4)\,\mathrm{keV} \end{aligned}$$

where the errors in brackets give an estimate of the spread between theories. Combining

these width estimates with the experimental branching ratios yields the results in Table 8.

Γ_{had} (keV)	EXPERIMENT	LO-QCD
$^3P_0$	> 340	$\simeq 550$
$^3P_1$	81 ± 25	$\simeq 30$
$^3P_2$	147 ± 47	$\simeq 146$

TABLE 8
Comparison of the ^3P_J widths as determined from experimental branching ratios with theoretical input with lowest order QCD predictions.[56] Note that the predictions for the states with spin $J = 0, 2$ are more reliable than the one for $J = 1$ due to the different decay mode of the latter state (see text).

Also given in Table 8 are lowest order QCD predictions. Barbieri *et al.*[56] calculated the two gluon decay width of the $^3P_0$ and $^3P_2$ states in lowest order and including radiative corrections.[57] The annihilation rate of the $^3P_1$ state was also estimated by Barbieri *et al.*[56] Although this state can decay into three gluons, the leading contribution results from a $gq\bar{q}$ decay. With estimates[58] on the derivative of the ^3P wave function and a value[11] of $\alpha_s = 0.165 \pm 0.005$ the predictions stated in Table 8 are obtained. The overall agreement between data and theory is striking given that we use theoretical input for the P wave function and the radiative width. It is certainly much better than the predictions for the corresponding $c\bar{c}$ P-states. The failure of this QCD calculation in the charmonium system is assumed to be due to relativistic and wave-function effects. These effects should be much smaller in the heavier $b\bar{b}$ system as the b quarks here are more non-relativistic. It is therefore of great importance to measure more accurately the hadronic width of the P states, in particular the $^3P_0$ width. Second order QCD predicts for the ratio

$$\frac{\Gamma(0^{++} \rightarrow hadrons)}{\Gamma(2^{++} \rightarrow hadrons)} = \frac{15}{4}(1 + 9.5\frac{\alpha_s}{\pi})$$

which, evaluated with the above given value of α_s, yields $\Gamma_{0^{++}}/\Gamma_{2^{++}} = 5.6$ to be compared to the lowest order prediction of $15/4 = 3.7$. The current experimental limit on this ratio is > 1.6, insufficient to test even the lowest order QCD calculation.

SUMMARY

The $\Upsilon(1S)$ states discussed here have been shown to be a well suited testing ground for the theory of strong interactions, QCD. Theoretical predictions are much more reliable for

the bottonium states than for the charmonium system, and thus better agreement is obtained between data and theory. Results are presented on radiative decays of the $\Upsilon(1S)$ and $\Upsilon(2S)$ resonances and the mass spectrum of the ^3P_J states.

Radiative decays from the $\Upsilon(1S)$ allow to search for the spin-singlet $^1S_0$ state of bottonium and for new states in the form of gluonium, supersymmetric particles or Higgs bosons. Considerable excitement was caused by evidence for a particle called ς found in 1984. Since then much more data was taken by all experiments operating at CESR and DORIS. Given all the negative results the existence of the ς seems very unlikely. The $^1S_0$ state has not yet been seen, and it is expected that significantly more data are needed to allow its discovery. The search for the Higgs boson has yielded a lower limit on its mass of 2 GeV, still far away from the theoretically lower limit of 7 GeV.

The ^3P_J states have been observed in radiative decays from the $\Upsilon(2S)$. A very high precision in mass determination of better than 10^{-4} has been achieved. In addition, the spins of the ^3P_J have been measured to be consistent with the expectation from potential models. The fine-structure splitting between these states yields information on the force acting between quarks. Based on this splitting it is shown that models inspired by QCD possess predictive powers superior to purely phenomenological approaches: a clear success for the potentials based on QCD which incorporate one-gluon exchange, asymptotic freedom and linear confinement. In comparison with charmonium the splittings also indicate the approach of the spin dependent potentials to the perturbative regime.

Of great importance for the future will be the discovery of the $^1P_1$ and the $^1S_0$ state. They will reveal the hyperfine part of the spin force, accessible otherwise only with a much heavier quarkonium system. As long as the $t\bar{t}$ system is not available, a precision study of the $2\,^3P_J$ states and the leptonic widths of all $^3S_1$ states are of high priority. They will allow an accurate determination of the scale parameter of QCD, $\Lambda_{\overline{MS}}$. Due to its high mass and narrow width the $\Upsilon(1S)$ state offers itself as a unique laboratory for the search for unexpected effects within or beyond the Standard Model. Although theoretical calculations are not free of problems, it is hoped that advances e.g. in the lattice gauge theories will be made in the near future to allow an even more quantitative comparison between theory and experiment.

ACKNOWLEDGEMENTS

I am indepted to my many colleagues in the Crystal Ball collaboration for many interesting and fruitful discussions on the material presented here. Thanks also to the ARGUS, CLEO and CUSB collaborations for communicating some of their material prior to publication. Finally I would like to acknowledge the hospitality received at DESY.

REFERENCES

1. S.L. Glashow, *Nucl. Phys.* **22** (1961) 579;
   S. Weinberg, *Phys. Rev. Lett.* **19** (1967) 1264;
   A. Salam in Elementary Particle Theory, ed. by N. Swartholm, p. 367
   (Almquist and Wiksell, Stockholm, 1968).

2. H. Fritsch and M. Gell-Mann, Proc. XVI Intl. Conf. on High Energy
   Physics, Vol. 2, p. 135 (Chicago, 1972);
   H. Fritsch, M. Gell-Mann and H. Leutwyler, *Phys. Lett.* **47B** (1973) 365;
   H.D. Politzer, *Phys. Rev. Lett.* **30** (1973) 1346;
   D.J. Gross and F. Wilczek *Phys. Rev.* **D8** (1973) 3633;
   S. Weinberg, *Phys. Rev. Lett.* **31** (1973) 494.

3. H. Fritsch and P. Minkowski, *Nuovo Cim.* **30A** (1975) 393;
   R.L. Jaffe and K. Johnson, *Phys. Lett.* **60B** (1976) 201;
   T. Barnes, *Zeit. Phys.* **C10** (1981) 275;
   C.E. Carlson, J.J. Coyne, P.M. Fishbane, F. Gross
   and S. Meshkov, *Phys. Lett.* **99B** (1981) 353.

4. J. Wess and B. Zumino, *Nucl. Phys.* **B78** (1974) 1;
   S. Ferrara and B. Zumino, *Nucl. Phys.* **B79** (1974) 413;
   P. Fayet, *Phys. Lett.* **69B** (1977) 489;
   F. Farrar and P. Fayet, *Phys. Lett.* **76B** (1978) 575.

5. J. Ellis, M.K. Gaillard and D.V. Nanopoulos, *Nucl. Phys.* **B106** (1976) 292.

6. D. Andrews *et al.*, *Nucl. Instr. Methods* **211** (1983) 47.

7. P. Franzini and J. Lee-Franzini, *Phys. Rep.* **81** (1982) 239.

8. A. Drescher *et al.*, *Nucl. Instr. Methods* **205** (1983) 125;
   M. Danilov *et al.*, *Nucl. Instr. Methods* **217** (1983) 153.

9. E.D. Bloom and C.W. Peck, *Ann. Rev. Nucl. Part. Sci.* **33** (1983) 143;
   M. Oreglia *et al.*, *Phys. Rev.* **D25** (1982) 2259.

10. T. Appelquist and H.D. Politzer, *Phys. Rev.* **D12** (1975) 1404
    and *Phys. Rev. Lett.* **34** (1975) 43;
    R. Barbieri, R. Gatto and E. Remiddi, *Phys. Lett.* **61B** (1976) 465;
    A. DeRujula and S.L. Glashow, *Phys. Rev. Lett.* **34** (1975) 46.

11. P.B. Mackenzie and G.P. Lepage, *Phys. Rev. Lett.* **47** (1981) 1244;
    S.J. Brodsky, G.P. Lepage and P.B. Mackenzie, *Phys. Rev.* **D28** (1983) 228.

12. D.W. Duke and R.G. Roberts, *Phys. Rep.* **120** (1985) 275.

13. R.D. Schamberger *et al.*, *Phys. Lett.* **138B** (1984) 225;
    P. Avery *et al.*, CLNS-83/582 (1983).

14. B. Guberina and J.H. Kühn, *Lett. Nuovo Cimento* **32** (1981) 295;
    J.G. Körner, J.H. Kühn, M. Krammer and H. Schneider, *Nucl. Phys.* **B229** (1983) 115;
    G.W. Intemann, *Phys. Rev.* **D27** (1983) 2755.

15. J.F. Donoghue and H. Gomm, *Phys. Lett.* **122B** (1983) 309;
    A. Billoire, R. Lacaze, A. Morel and H. Navelet, *Phys. Lett.* **80B** (1979) 381.

16. S. Weinberg, *Phys. Rev. Lett.* **36** (1976) 294;
    A.D. Linde, *Phys. Lett.* **70B** (1977) 306.

17. F. Wilczek, *Phys. Rev. Lett.* **39** (1977) 1304.

18. P.H. Frampton and W.W. Wada, *Phys. Rev.* **D19** (1979) 271;
    H.E. Haber, G.L. Kane and T. Sterling, *Nucl. Phys.* **B161** (1979) 493;
    M.I. Vysotsky, *Phys. Lett.* **97B** (1980) 159;
    J. Ellis, K. Enqvist, D.V. Nanopoulos and S. Ritz, CERN-TH.4143 (1985).

19. J.F. Donoghue and L.F. Li, *Phys. Rev.* **D19** (1979) 945;
    H.E. Haber and G.L. Kane, *Phys. Lett.* **135B** (1984) 196;
    L. Lane, S. Meshkov and F. Wilczek, *Phys. Rev. Lett.* **53** (1984) 1718;
    S. Glashow and M. Machacek, *Phys. Lett.* **145B** (1984) 302;
    H. Georgi, A. Manohar and G. Moore, *Phys. Lett.* **149B** (1984) 234;
    R.S. Willey, *Phys. Rev. Lett.* **52** (1984) 585.

20. W.Y. Keung, *Phys. Rev.* **D28** (1983) 1129;
    J. Zuk, G.C. Joshi and J.W.G. Wignall *Phys. Rev.* **D28** (1983) 1706;
    J.H. Kühn and S. Ono, *Phys. Lett.* **142B** (1984) 436;
    D.V. Nanopoulos, S. Ono and T. Yanagida, *Phys. Lett.* **137B** (1984) 363.

21. E. Eichten, K. Gottfried, T. Kinoshita, K.D. Lane and T.M. Yan,
    Phys. Rev. **D17** (1978) 3090 and *Phys. Rev.* **D21** (1980) 203;
    T. Appelquist, R.M. Barnett and K. Lane, *Ann. Rev. Nucl. Part. Sci.* **28** (1978) 387.

22. A.D. Steiger, *Phys. Lett.* **129B** (1983) 335.

23. R. McClary and N. Byers, *Phys. Rev.* **D28** (1983) 1692.

24. C.W. Peck *et al.*, SLAC-PUB-3380 and DESY 84-064(1984).

25. E.D. Bloom, Crystal Ball Collaboration, SLAC-PUB-3686 and Proceedings
    of the 5^{th} Topical Workshop on Proton Antiproton Collider Physics,
    St. Vincent, Italy, March 1985;
    S.T. Lowe, Crystal Ball Collaboration, SLAC-PUB-3683 and Proceedings
    of the XX^{th} Rencontre de Moriond, Les Arcs, France, March 1985.

26. J. Lee-Franzini, CUSB Collaboration, Proceeding of the 5^{th} International
    Conference on Physics in Collision, Autun, France, July 1984.

27. D. Peterson, CLEO Collaboration, Proceedings of the International Conference
    on Hadron Spectroscopy, College Park, Maryland, April 1985.

28. H. Albrecht *et al.*, DESY 85-083 (1985), submitted to Zeit. Phys.

29. S.H.H. Tye and C. Rosenfeld, *Phys. Rev. Lett.* **53** (1984) 2215.

30. S.W. Otto and J.D. Stack, *Phys. Rev. Lett.* **52** (1984) 2328.

31. C. Quigg and J.L. Rosner,*Phys. Rep.* **56** (1979) 167.

32. A. Martin, *Phys. Lett.* **93B** (1980) 338 and *Phys. Lett.* **100B** (1981) 511;
    K.J. Miller and M.G. Olsson, *Phys. Lett.* **109B** (1982) 314.

33. G. Bhanot and S. Rudaz, *Phys. Lett.* **78B** (1978) 119.

34. H. Krasemann and S. Ono, *Nucl. Phys.* **B154** (1978) 283.

35. J.L. Richardson, *Phys. Lett.* **82B** (1979) 272.

36. W. Buchmüller, G. Grunberg and S.H.H. Tye, *Phys. Rev. Lett.* **45** (1980) 103
    and erratum *Phys. Rev. Lett.* **45** (1980) 587;
    W. Buchmüller and S.H.H. Tye, *Phys. Rev.* **D24** (1981) 132.

37. J.S. Kang and H.J. Schnitzer, *Phys. Rev.* **D12** (1975) 842.

38. E. Eichten and F. Feinberg, *Phys. Rev. Lett.* **43** (1979) 1205
and *Phys. Rev.* **D23** (1981) 2724.

39. D. Gromes, *Zeit. Phys.* **C26** (1984) 401.

40. M.G. Olsson, *Phys. Rev.* **D28** (1983) 1223;
M.E. Peskin, SLAC-PUB-3273 and Proceedings of the 11^{th} SLAC Summer Institute on Particle Physics, Stanford, July 1983.

41. C. Klopfenstein *et al.*, *Phys. Rev. Lett.* **51** (1983) 160;
F. Pauss *et al.*, *Phys. Lett.* **130B** (1983) 439.

42. P. Haas *et al.*, *Phys. Rev. Lett.* **52** (1984) 799.

43. H. Albrecht *et al.*, DESY 85-068 (1985), submitted to Phys. Lett.

44. R. Nernst *et al.*, *Phys. Rev. Lett.* **54** (1985) 2195;
W. Walk *et al.*, SLAC-PUB-3575 and DESY 85-019, submitted to Phys. Rev. D.

45. T. Skwarnicki, Crystal Ball Collaboration, DESY 85-042 (1985) and Proceedings of the 22^{nd} Rencontre de Moriond, Les Arcs, France, March 1985.

46. L.S. Brown and R.N. Cahn, *Phys. Rev.* **D13** (1976) 1195.

47. Particle Data Group: Review of Particle Properties, *Rev. Mod. Phys.* **56,II** (1984).

48. S.N. Gupta, S.F. Radford and W.W. Repko, *Phys. Rev.* **D26** (1982) 3305
and *Phys. Rev.* **D30** (1984) 2424.

49. W. Buchmüller, *Phys. Lett.* **112B** (1982) 479 and Proceedings of the Moriond Workshop on New Flavors, Les Arcs, France, January 1982.

50. A. Khare, *Phys. Lett.* **98B** (1981) 385.

51. P. Moxhay and J.L. Rosner, *Phys. Rev.* **D28** (1983) 1132.

52. H. Grotch, D.A. Owen and K.L. Sebastian, *Phys. Rev.* **D30** (1984) 1924.

53. M. Bander, B. Klima, U. Maor and D. Silverman, *Phys. Rev.* **D29** (1984) 2038
and *Phys. Lett.* **134B** (1984) 258.

54. S. Ono and N.A. Törnqvist, *Phys. Rev.* **D29** (1984) 110 and erratum
Phys. Rev. **D29** (1984) 2136 and *Zeit. Phys.* **C23** (1984) 59.

55. K. Hagiwara, S. Jacobs, M.G. Olsson and K.G. Miller, *Phys. Lett.* **131B** (1983) 455.

56. R. Barbieri, R. Gatto and R. Kögerler, *Phys. Lett.* **60B** (1976) 183;
R. Barbieri, R. Gatto and E. Remiddi, *Phys. Lett.* **61B** (1976) 465.

57. R. Barbieri, M. Caffo, R. Gatto and E. Remiddi, *Phys. Lett.* **95B** (1980) 93;
R. Barbieri, R. Gatto and E. Remiddi, *Phys. Lett.* **106B** (1981) 497.

58. M.G. Olsson, A.D. Martin and A.W. Peacock, *Phys. Rev.* **D31** (1985) 81.